International Journal of Bifurcation and Chaos, Vol. 20, No. 2 (2010) 341–347

DOI: 10.1142/S021812741002579X

EMBRYONIC SOMITE FORMATION GENERATED BY GENETIC NETWORK OSCILLATIONS WITH NOISE

KARINA I. MAZZITELLO, CONSTANCIO M. ARIZMENDI*,
ALVARO L. SALAS BRITO† and HILARY G. E. HENTSCHEL‡
CONICET-Facultad de Ingeniería, Universidad Nacional de Mar del Plata, Juan B. Justo 4302, B7608FDQ Mar del Plata, Argentina
**Facultad de Ingeniería, Universidad Nacional de Mar del Plata, Juan B. Justo 4302, B7608FDQ Mar del Plata, Argentina*
†*Univ Autonoma Metropolitana Azcapotzalco, Lab Sistemas Dinam, Coyoacan 04000, DF Mexico*
‡*Department of Physics, Emory University, Atlanta, Georgia 30322, USA*

Received November 14, 2008; Revised April 15, 2009

In most vertebrate species, the body axis is generated by the formation of repeated transient structures called somites. This spatial periodicity in somitogenesis has been related to the genetic network oscillations in certain mRNAs and their associated gene products in the cells forming the presomitic mesoderm. The current molecular view of the mechanism underlying these oscillations involves negative-feedback regulation at transcriptional and translational levels. The spatially periodic nature of somite formation suggests that the genetic network involved must display intracellular oscillations that interact with a longitudinal positional information gradient, called determination front, down the axis of vertebrate embryos to create this spatial patterning. Here, we consider a simple model for diploid cells based on this current biological picture considering gene regulation as a noisy process relevant in a real developmental situation and study its consequences for somitogenesis. Comparison is made with the known properties of somite formation in the zebrafish embryo.

Keywords: Genetic networks; cellular biology; delay systems; somitogenesis.

1. Introduction

In the classic view of cellular biology, cells are simply a product of genetic and environmental conditions, and all differences between individual cells can be attributed to one or both of these factors. Recent work, however, suggests that when grown in the same environment, cells from genetically identical populations can exhibit very different behaviors. Why some cells remain in one phenotypic state whereas others switch to a different one, and what the molecular processes are determining their fate, remain open questions.

The case of somitogenesis, the generation of somites from a nascent vertebrate, is a good example since it deals with structure formation in an embryo, where cells initially with the same genes result in different phenotypic states. Somites are transient structures forming a periodic growing pattern that starts from the head (anterior) and that extends to the tail (posterior) side of a developing vertebrate embryo ultimately giving rise to both the segmented vertebral column and the musculature. Formation of somites is a rhythmic process characteristic of the species at given temperature.

For instance, in the chicken embryo one pair of somites is formed every 90 min at 37°C and in the zebrafish one pair is formed roughly every 30 min at 28°C. The total number of somites produced is conserved within a given species typically somewhere between 50 to 70 pairs of somites form on each side of the anterior–posterior (AP) axis, but can vary dramatically between species, thus the zebrafish develops 30 pairs of somites. As new somites bud from the anterior end of the presomitic mesoderm (PSM) that extends back to the primitive streak and tail bud, new cells are added at the posterior end by cell division from the tail bud keeping the size of the PSM constant as new somites are generated.

A number of models have been proposed to address the mechanisms underlying the generation of somitogenesis periodic patterns [Baker *et al.*, 2006; Aulhela & Pourquié, 2006; Pourquié, 2003; Aulhela & Herrmann, 2004; Palmeirim *et al.*, 1997; Rida *et al.*, 2004]: The Clock and Wavefront model proposed by Coke and Zeeman in 1976 and Meinhardt's Reaction Diffusion model are perhaps the most known. Both models suppose that oscillations of genes and gene products occur in the cells of the PSM from which the somites are derived (Fig. 1). The Clock and Wavefront model postulates the existence of a longitudinal positional information gradient down the axis of vertebrate embryos. This gradient interacts with the cellular oscillator stopping the oscillations and producing a rapid change in locomotory and adhesive behavior of cells when they form somites [Dale, & Pourquié, 2000; Drubrulle *et al.*, 2001]. The oscillation in the PSM

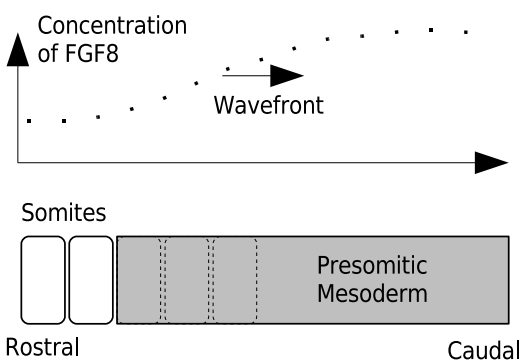

Fig. 1. Schematic representation of somitogenesis within the Clock and Wavefront model. Gene and gene product concentrations in the cells of PSM experience temporal oscillations. A longitudinal positional information gradient (see top of the diagram) stops the oscillations of the genetic network. The somites form in a rostral to caudal order as the wavefront advances from head to tail.

is the somite clock, and the moving interfaces at the anterior end of the PSM where the positional information reaches a critical value is called the wavefront. It is the interaction between the clock phase and the positional information that controls somitogenesis.

Recently, a deterministic one-dimensional model has been introduced based on the Clock and Wavefront model combined with key ingredients of the known biology for zebrafish embryo [Mazzitello *et al.*, 2008]. The deterministic model uses the recent proposal for the mechanism producing the intracellular oscillations as due to delays in the synthesis of mRNA focusing specifically on the zebrafish genes her1 and her7 and their gene products the protein molecules Her1 and Her7 [Lewis, 2003]. The position of the wavefront was shown to be defined by the concentration of the secreted factor Fgf8 whose mRNA is expressed in a graded fashion in the caudal PSM [Pourquié, 2003]. At low Fgf8 concentration, cell arrangement becomes more compact and the epithelialization process underlying somite formation begins [see Fig. 1]. In the deterministic model the signal created by the Fgf8 concentration interacts with the clock phase leading to cell differentiation and somite formation.

Genetic networks, involved in somite formation, create complex temporal distributions of intracellular proteins in cells, as transcription step in protein synthesis is essentially a stochastic process because of the small number of molecules involved in the cells. In this work, the effect of noise on the genetic clock and on the spatial pattern of somites is studied. An important characteristic of the zebrafish is that, although it is generally diploid, by means of genetic manipulations, haploid embryos can be generated. The treatment of noise depends on the diploid or haploid character of the cells. Haploid cells were considered previously [Mazzitello *et al.*, 2008]. The general case of the stochastic effect for diploid cells is studied here. The paper is outlined as follows: Sec. 2 is devoted to description and mathematical formulation of the genetic network model for diploid cells. The temporal oscillations and the spatial pattern of the gene concentrations obtained are shown in Sec. 3. Finally a conclusion and discussion is presented in Sec. 4.

2. Genetic Network Model

A somitogenesis clock, linked to the vertebrate embryo segmentation process has been uncovered

recently in zebrafish [Saga & Takeda, 2001]. The genes her1 and her7 show oscillatory expressions in the presomitic mesoderm (PSM) and their oscillations are in synchrony by the Notch signaling. The expressions of both genes are thought to be enhanced by Notch signaling and negatively regulated by their associated Her1 and Her7 proteins [Aulhela & Herrmann, 2004].

Sustained oscillations (necessary for the somitogenesis clock) of gene expressions and their associated proteins can be obtained via a negative delayed feedback [Elowitz & Leibler, 2000; Morelli & Jülicher, 2007], simply by taking account of the delays involved in the synthesis of mRNA and proteins: the time between initiation of transcription and arrival of the mature mRNA molecule in the cytoplasm T_m and the delay, T_p, between the initiation of translation and the emergence complete functional protein molecule.

Although the PSM is a three-dimensional structure and a mediolateral spread of expression waves has been described in chicks [Freitas *et al.*, 2001] for the purposes of this study only the anteroposterior axis is of interest.

The model thus consists initially of a linear array of N_{start} cells that represents the starting size of the PSM with intracellular oscillators driven by the her1 and her7 genes and their associated gene product proteins. The oscillations between nearest-neighbor cells are coupled and synchronized via Notch signaling [Oates & Ho, 2002]. The cell–cell communication is produced by the deltaC gene product Notch crossing the cell membrane wall.

In each cell the gene mRNA concentrations m_k for the genes $k \equiv \text{her1}, \text{her7}, \text{deltaC}$ and their associated gene products with protein concentrations p_k obey the sets of coupled kinetic equations (see [Lewis, 2003; Mazzitello, 2008]):

$$\frac{dp_k^i}{dt}(t) = am_k^i(t - T_{p_k}) - bp_k^i(t), \tag{1}$$

$$\frac{dm_k^i}{dt}(t) = \frac{1}{nn}\sum_{i'=1}^{nn} f_k(p_{\text{her1}}^i(t - T_{m_k}), p_{\text{her7}}^i(t - T_{m_k}), p_{\text{deltaC}}^{i'}(t - T_{m_k})) - cm_k^i(t), \tag{2}$$

where i denotes the cell position in the linear array; i' goes from 1 to nn, the number of nearest neighbor cells of i (nn can be 1 if i is at an end or 2 otherwise); T_{m_k} is the delay time from initiation of transcription to export of the mature mRNA m_k into the cytosol; T_{p_k} is the delay between the initiation of translation and the emergence of the complete protein molecule p_k; a represents the protein p_k synthesis rate per mRNA molecule; b is the rate of protein p_k degradation; c is the rate of mRNA m_k degradation; while the function f_k represents the rate of production of new mRNA molecules m_k (see Table 1).

Genes are regulated by a set of proteins called transcription factor with specific function of turning genes on and it off. The way to do this is by binding to specific sequences of DNA and can be classified as either activators which enhance the rate of genes transcription over its basal rate or repressors which decrease the rate of genes transcription when they bind to a given sequence of DNA. In a cell, the number of molecules involved in protein synthesis is small and the binding and dissociation of a gene regulatory protein to and from its site on DNA molecule is a stochastic process. Thus, the functions f_k are given by:

$$f_{\text{her1/7}}(p_{\text{her1}}^i(t'), p_{\text{her7}}^i(t'), p_{\text{deltaC}}^{i'}(t')) = K_{\text{her1/7}}\xi_{\text{her1/7}}^i(t')\frac{[2 - \eta_{\text{her1/7}}^{i'}(t')]}{4} \tag{3}$$

$$f_{\text{deltaC}}(p_{\text{her1}}^i(t'), p_{\text{her7}}^i(t'), p_{\text{deltaC}}^{i'}(t')) = \frac{K_{\text{deltaC}}\xi_{\text{deltaC}}^i(t')}{2}, \tag{4}$$

where $K_{\text{her1/her7}}$ and K_{deltaC} are the rates of transcription in the absence of inhibition and activation, respectively. $\xi_{\text{her1/7}}, \eta_{\text{her1/7}}$ and ξ_{deltaC}, are random variables rv taking value $0, 1$ or 2 according to whether neither, one or both of the two sites in a diploid cell are in the unoccupied state, respectively. We consider the occupied state as the state zero because occupancy in most of the situations corresponds to inhibition. These random variables take a value at given time t conditioned by the values the random variables take at an earlier time $t' = t - T_{m_k}$ when synthesis of $m_k(t)$ begins ($k = \text{her1}, \text{her7}, \text{deltaC}$). Thus, for example, the probability that both of the two sites in a diploid cell are unoccupied at time $t + \Delta t$ if both at time t are occupied is the product p_{10}^2 of the single-gene transition probabilities from 0 occupied state at t to 1 unoccupied state at $t + \Delta t$, in each site. Generalizing, the probability $P_{\alpha\beta}^{\text{rv}}$ that the random variable rv ($rv = \xi_{\text{her1/7}}, \eta_{\text{her1/7}}, \xi_{\text{deltaC}}$) takes value α ($\alpha = 0, 1, 2$) at time $t + \Delta t$ if the state at time t is β ($\beta = 0, 1, 2$) can be expressed in terms

Table 1. List of parameters and functions and their relationships with gene mRNA concentration m_k and their associated gene products with protein concentrations p_k ($k = \text{her1}, \text{her7}, \text{deltaC}$).

Main Variables	Parameters and Functions	Descriptions of Parameters and Functions
	T_{m_k}	Delay time between the initiation of transcription and arrival of a m_k molecule in the cytoplasm.
m_k	c	Rate of mRNA m_k degradation.
	K_k	Rate transcription in absence of inhibition and/or activation.
	f_k	Rate of mRNA m_k production.
	$\xi_k, \eta_{\text{her1/7}}$	Random functions related to the occupation by proteins of sites in diploid cells.
	$P^{\text{rv}}_{\alpha\beta}$	Probability associated to the random function $rv(\text{rv} = \xi_k, \eta_{\text{her1/7}})$.
	$p^{\text{rv}}_{\alpha\beta}$	Occupation probability of sites in a diploid cell.
p_k	$k^{\text{rv}}_{\text{on}}, k^{\text{rv}}_{\text{off}}$	Rate constant for protein binding (on) or dissociation (off) from their regulatory DNA binding sites.
	p^{crit}_k	Critical number of proteins per cell.
	T_{p_k}	Delay between the initiation of translation and the emergence of a complete protein p_k.
	a	Protein synthesis rate per m_k molecule.
	b	Rate of protein degradation p_k.

of the single-gene transition probabilities as follows:

$$P^{\text{rv}}_{\alpha\beta} = \frac{3+(-1)^{\beta}}{4} \sum_{\gamma,\delta,\rho,\nu=0}^{1} p^{\text{rv}}_{\gamma\delta} p^{\text{rv}}_{\rho\nu}, \quad \text{with } \gamma+\rho=\alpha \quad \text{and} \quad \delta+\nu=\beta. \tag{5}$$

$p^{\text{rv}}_{\gamma\delta}$ represents the probability that a given site in a diploid cell takes the value γ ($\gamma = 0, 1$) at time $t + \Delta t$ if it had values δ ($\delta = 0, 1$) at time t. Specifically, the probability that a site takes value 1 (unbound) at time $t + \Delta t$ depends on the state of the appropriate regulatory site at time t (bound or unbound).

$$p^{\text{rv}}_{10}(t+\Delta t) = 1 - F^{\text{rv}}(t+\Delta t) | (F^{\text{rv}}(t) = 0), \quad \text{if the regulatory site is bound at } t \tag{6}$$

$$p^{\text{rv}}_{11}(t+\Delta t) = F^{\text{rv}}(t+\Delta t) | (F^{\text{rv}}(t) = 1), \quad \text{if the regulatory site is unbound at } t \tag{7}$$

where $F^{\text{rv}}(t)$ is the probability that the regulatory site is free. This probability obeys the master equation

$$\frac{dF^{\text{rv}}}{dt} = k^{\text{rv}}_{\text{off}}(1 - F^{\text{rv}}) - k^{\text{rv}}_{\text{on}} F^{\text{rv}}. \tag{8}$$

These kinetic coefficients are discussed in [Lewis, 2003] (Supplemental Data), where $k^{\text{rv}}_{\text{on}}$ the rate constant for protein binding is a Michaelis–Menten function of the protein concentrations, while $k^{\text{rv}}_{\text{off}}$ is the rate constant for dissociation of the proteins from their regulatory DNA binding sites (typically biologically $k^{\text{rv}}_{\text{off}} \approx 1\text{min}^{-1}$ implying a mean lifetime of about 1 min for the bound state). The steady state of master equation is $F^{\text{rv}} = k^{\text{rv}}_{\text{off}}/(k^{\text{rv}}_{\text{off}} + k^{\text{rv}}_{\text{on}})$.

In order to reproduce oscillatory transcription with minimum regulations we take into account only essential regulations, i. e. proteins experimentally observed behaving as transcription factors [Mazzitello *et al.*, 2008]. To represent the action of protein products of her1 and her7, regulation by homodimers of Her is not essential for the cyclic transcription. Somite segmentation and clock gene expression is disrupted in the absence of either Her1 or Her7, suggesting that Her1/Her7 heterodimer plays the central role [Giudicelli *et al.*, 2007]. For the delta expression, consideration of Her dependent repression is sufficient and other regulation term is not essential [Gajewsky *et al.*, 2003]. Transcripts are assumed to be initiated at zero rate when repressor (activator) is bound (unbound) and at maximal rate when it is unbound (bound). Then, considering only essential regulations, we must have

$$K_{\text{her1/7}} F^{\xi_{\text{her1/7}}, \eta_{\text{her1/7}}} = \frac{K_{\text{her1/7}}}{(1 + \phi_{\text{her1}}\phi_{\text{her7}})} \tag{9}$$

$$K_{\text{deltaC}} F^{\xi_{\text{deltaC}}} = \frac{K_{\text{deltaC}}\phi_{\text{deltaC}}}{(1 + \phi_{\text{deltaC}})}, \tag{10}$$

where $\phi_k^i(t) = p_k^i(t)/p_k^{\rm crit}$. $p_{\rm her1/7}^{\rm crit}$ is the critical number of molecules of Her1 or Her7 protein per cell, for inhibition of transcription, while $p_{\rm deltaC}^{\rm crit}$ represents the critical number of Notch molecules required for activation of transcription. Thus, the mean rates of transcript initiations in our stochastic system will then have the same dependence on p_k as should be postulated for a deterministic system with minimum regulations [Mazzitello *et al.*, 2008].

Using the steady state expression obtained above and Eqs. (9) and (10), $k_{\rm on}^{\eta_{\rm her1/7}} = k_{\rm off}^{\eta_{\rm her1/7}}\phi_{\rm her1}\phi_{\rm her7}$ and $k_{\rm on}^{\xi_k} = k_{\rm off}^{\xi_k}/\phi_{\rm deltaC}$, with $\xi_k = \xi_{\rm her1/7}$ or $\xi_{\rm deltaC}$. Solving the master equation with $k_{\rm on}^{\rm rv}$ previously obtained results in the forms $P^{\rm rv}(t+\Delta t) = u^{\rm rv}(1-\exp[-v\Delta t]) + P^{\rm rv}(t)\exp[-{\rm v}^{\rm rv}\Delta t]$, where $v^{\rm rv} = (k_{\rm off}^{\rm rv}+k_{\rm on}^{\rm rv})$ and $u^{\rm rv} = k_{\rm off}^{\rm rv}/v^{\rm rv}$. Inserting these solutions in Eqs. (6) and (7) one obtains

$$p_{10}^{\rm rv}(t+\Delta t) = u^{\rm rv}(1-e^{[-v^{\rm rv}\Delta t]}),$$
if the regulatory site is bound at t (11)

$$p_{11}^{\rm rv}(t+\Delta t) = u^{\rm rv}(1-e^{[-v^{\rm rv}\Delta t]}) + e^{[-v^{\rm rv}\Delta t]},$$
if the regulatory site is unbound at t (12)

where $rv = \xi_{\rm her1/7}$, $\eta_{\rm her1/7}$ or $\xi_{\rm deltaC}$.

Following the same procedure, the probability that a given site in a diploid cell takes the value 1 (bound) at time $t+\Delta t$ is given by

$$p_{01}^{\rm rv}(t+\Delta t) = (1-u^{\rm rv})(1-e^{[-v^{\rm rv}\Delta t]}),$$
if the regulatory site is unbound at t (13)

$$p_{00}^{\rm rv}(t+\Delta t) = 1-u^{\rm rv}(1-e^{[-v^{\rm rv}\Delta t]}),$$
if the regulatory site is bound at t. (14)

In summary, the temporal evolution of p_k and m_k for the diploid cells of the linear array are calculated integrating Eqs. (1) and (2), while the function f_k that represents the rate of production of new mRNA molecules m_k is given by Eqs. (3) and (4). The random variables $\xi_{\rm her1/7}$, $\eta_{\rm her1/7}$ and $\xi_{\rm deltaC}$ are obtained through Eq. (5), where the products of probabilities involved are calculated using Eqs. (11)–(14) (a list of the parameters, variables and funtions is given in Table 1). Noise level is given by the value of the rate constant for dissociation of proteins $k_{\rm off}^{\rm rv}$ and in the limit of large $k_{\rm off}^{\rm rv}$ the noise is annulled (i.e. $\langle\xi_{\rm her1/7,deltaC}\rangle_{k_{\rm off}^{\xi}\to\infty} = 2/(1+\phi_{\rm her1}\phi_{\rm her7})$, $\langle\eta_{\rm her1/7}\rangle_{k_{\rm off}^{\eta}\to\infty} = 2/(1+\phi_{\rm deltaC})$).

3. Simulation and Results

In Fig. 2, concentrations of $m_{\rm her1}$ for any cell of the PSM before somite formation begins versus time are compared for: a typically biologic noise level ($k_{\rm off}^{\rm rv} = 1\,{\rm min}^{-1}$, with rv = $\xi_{\rm her1/7}, \eta_{\rm her1/7}, \xi_{\rm deltaC}$), a higher noise level ($k_{\rm off}^{\rm rv} = 0.1\,{\rm min}^{-1}$) and a low noise level ($k_{\rm off}^{\rm rv} = 10\,{\rm min}^{-1}$). The parameter values a, b, c, K, $p_{\rm k}^{\rm crit}$, T_{m_k}, and $T_{p_{\rm k}}$ are specified in the figure caption and are in the ranges estimated in [Lewis, 2003] using biological data. A random variability in the amplitude and shape of individual oscillation peaks can be seen for the results obtained with the two higher noise levels. In addition, as the amplitude of noise increases, the oscillations of $m_{\rm her1}$ lose periodicity. Nevertheless, the oscillations obtained with a typically biological noise level are synchronized with those obtained for a lower noise level and the period obtained is in good agreement with the observed period of 30 min for the zebrafish somite oscillator at 28°C.

To obtain a spatial pattern of protein and mRNA concentrations, we suppose at time $t = 0$ all the cells in the starting PSM, with an initial number of cells $N_{\rm start} = 100$, oscillating in phase affected by a noise level $k_{\rm off}^{\rm rv} = 1\ {\rm min}^{-1}$ and integrate Eqs. (1) and (2) for the time necessary to obtain

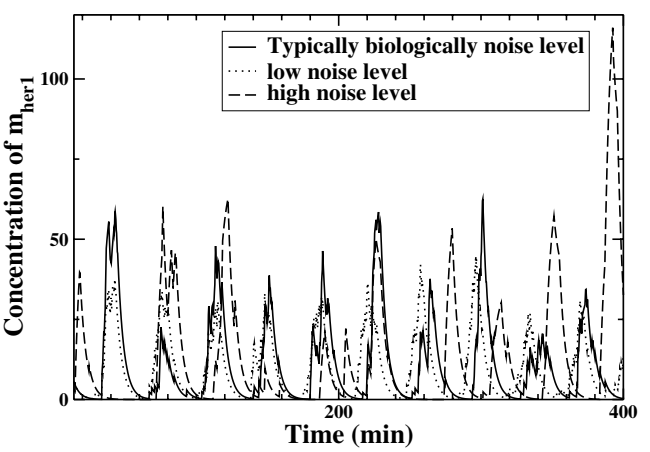

Fig. 2. Concentration of messenger mRNA molecules (number of molecules per cell) of gene her1 as a function of time for any cell of the linear array. Comparison of results obtained using different levels of noise: a low noise level (dotted line, $k_{\rm off}^{\rm rv} = 10\ {\rm min}^{-1}$), a typically biological noise level (solid line, $k_{\rm off}^{\rm rv} = 1$) and a higher noise level (dashed line, $k_{\rm off}^{\rm rv} = 0.1$). The parameter values are $a = 4.5$, $b = 0.23$, $c = 0.23$, $K_k = 33$ molecules per min, $p_{\rm her1/7}^{\rm crit} = 40$, $p_{\rm deltaC}^{\rm crit} = 1000$ molecules, $T_{m_{\rm her1}} = 10.2$, $T_{m_{\rm her7}} = 5.7$, $T_{m_{\rm deltaC}} = 16$ min, $T_{p_{\rm her1}} = 2.8$, $T_{p_{\rm her7}} = 1.7$, $T_{p_{\rm deltaC}} = 12$ min. The concentrations of protein and message molecules have the same behavior as the concentration of $m_{\rm her1}$ shown in this figure.

synchronous oscillations. The growth of the PSM is produced by mitosis experienced by the 20–40 last cells at posterior end of the linear array. During this process the transcription and translation of genes are arrested and cell division lasts at least 15 min [Horikawa *et al.*, 2006]. In order to simulate these experimental features during the division we assume the delay times are doubled and the synthesis rate of mRNAs and proteins is set to the halves. We calculate the rate of end cell division according to the measured growth rates [Holley, 2002] of one cell every 5 min. Thus, it generates sequentially along the antero-posterior axis the necessary cells for forming the future somites created at the anterior portion of the PSM, see Fig. 1. In our simulations, once the initial PSM has been obtained as a group of cells oscillating, the caudal motion of the wavefront starts. The wavefront velocity is given by the PSM growth rate of one cell every 5 min. We assume that the wavefront interacts with cells by stopping the oscillations. This effect has been studied in [Mazzitello *et al.*, 2008], a Hes6-related hairy/Enhancer of split-related gene, her13.2, that links FGF signaling to the Notch-regulated oscillation machinery was considered including a term to enhance the self-repression of her1 through formation of Her1-Her13.2 heterodimer complex. The observed spatial shift in the phases of different cells is thus obtained by the wavefront that advances to a rate of 5 min for cell catching different phases in the oscillations of the mRNA concentrations and their gene products. The simulation finishes in time $t = 900$ min and a somite regular pattern for the diploid cell model is found as shown in Fig. 3.

In order to test the validity of our model, we propose to perturb somitic pattern altering the segmentation clock period. The alteration of the segmentation clock period might be produced experimentally through modification of FGF8 concentration level in the PSM [Giudicelli *et al.*, 2007; Mazzitello *et al.*, 2008]. The dependance of the oscillation period on the FGF8 concentration level in the PSM is reflected because cells located in the region of high FGF8 concentration display longer period oscillations than those with low FGF8 concentration in order that the anterior PSM cells slow down and cease oscillations as they begin differentiation. According to our model, the variation of FGF8 concentration has an effect only on her1/7 messengers and proteins. The experimental prediction related to delay times

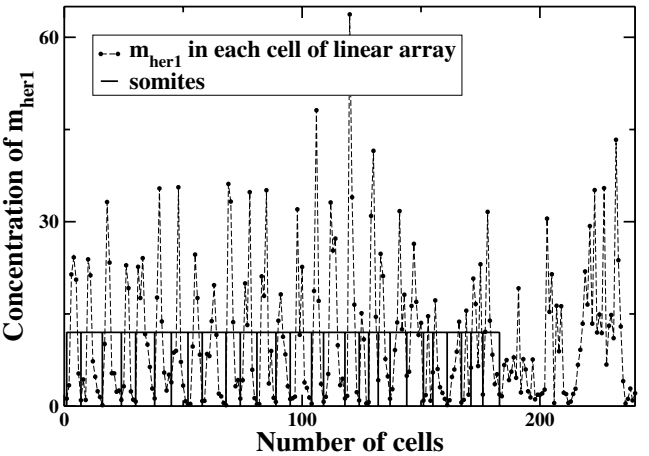

Fig. 3. Concentration of mRNA molecules (number of molecules per cell) of gene her1 as a function of cell number at the linear array. All the other concentrations of protein and mRNA molecules in the cells have the same qualitative behavior as the concentration of m_{her1} and were calculated with a typically biological noise level, $k_{\mathrm{off}}^{\mathrm{rv}} = 1.\ \mathrm{min}^{-1}$, and using the same parameter values as in Fig. 2 (see caption). The concentrations belonging to cells that were reached by the wavefront were frozen. At $t = 900$ min, 28 somites were formed.

dependence of our model is that when FGF8 concentration level increases, the delay times associated with her1/7 messengers and proteins will be reduced, the number of somites will increase, while the average somite size will decrease. This behavior associated with the decreasing of the delay times associated with her1/7 messengers and proteins will be obtained until a threshold in which the temporal oscillations are lost and the somitic pattern disappears [Lewis, 2003; Mazzitello *et al.*, 2008].

4. Conclusions

A variant of the multicellular genetic network model associated to zebrafish somitogenesis introduced in [Mazzitello *et al.*, 2008] to consider gene regulation as a noisy process in a situation of natural development is studied. An important characteristic of the zebrafish is that, although it is generally diploid, animals displaying a mutant phenotype can be generated from a single heterozygous parent by manipulation of the ploidy of the fertilized egg resulting in gynogenetic haploid embryos, which carry only a single maternal copy of each gene. The treatment of the noise is different for haploid and diploid cells because of the different number of sites in cells due to the transcription of mRNA molecules (two sites in diploid cells and only one site in haploid

cells). Although this difference may induce oscillatory behavior in different parameter ranges which may be important from a biological viewpoint, it will also be considered elsewhere. A model considering haploid cells were studied previously [Mazzitello *et al.*, 2008]. In this work the more general case of diploid cells is studied. We consider the binding and dissociation of gene regulatory proteins to and from DNA molecules as a stochastic process on a deterministic model. The specificity of this noise is different from the general intrinsic noise on stochastic delay systems that has been studied in recent works using the Gillespie algorithm [Barrio *et al.*, 2006; Galla, 2009]. A Hill function representing the action of transcription factors is used on these stochastic delay systems [Barrio *et al.*, 2006; Galla, 2009] instead of the binding and dissociation of the transcription factors to and from DNA molecules as a stochastic process used in this work.

Oscillations with a period in good agreement with the observed period of 30 min for the zebrafish somite oscillator at 28°C are obtained. In a similar way the presomitic pattern obtained for the typically biological noise level resembles in periodicity and in number of somites to the zebrafish presomitic pattern.

References

Aulhela, A. & Herrmann, B.G. [2004] "Segmentation in vertebrates: Clock and gradient finally joined," *Genes Dev.* **18**, 2060–2067.

Aulhela, A. & Pourquié, O. [2006] "On periodicity and directionality of somitogenesis," *Anat. Embryol. Rev.* doi 10.1007/s0029-006-0124-y.

Baker, R.E., Schnell, S. & Maini, P.K. [2006] "A clock and wavefront mechnism for somite formation," *Dev. Biol.* **293**, 116–126.

Barrio, M., Burrage, K., Leier A. & Tian, T. [2006] "Oscillatory regulation of Hes1: Discrete stochastic delay modelling and simulation," *PLoS Copm. Biol.* **2**, 1017–1030.

Dale, K.J. & Pourquié, O. [2000] "A clock-work somite," *BioEssays* **22**, 72–83.

Dubrulle, J., McGrew, M.J. & Pourquié, O. [2001] "FGF signalling controls somite boundary position and regulates segmentation clock control of spatiotemporal Hox gene activation," *Cell* **106**, 219–232.

Elowitz, M.B. & Leibler, S. [2000] "A synthetic oscillatory network of transcriptional regulators," *Nature* (*London*) **403**, 335–338.

Freitas, C., Rodrigues, S., Charrier, J., Teillet, M. & Palmeirim, I. [2001] "Evidence for medial/lateral specification and positional information within the presomitic mesoderm," *Development* **128**, 5139–5147.

Gajewski, M., Sieger, D., Alt, B., Leve, C., Hans, S., Wolff, C., Rohr, B.K. & Tautz, D., [2003] "Anterior and posterior waves of cyclic her1 gene expression are differentially regulated in the presomitic mesoderm of zebrafish," *Development* **130**, 4269–4278.

Galla, T. [2009] "Intrinsic fluctuations in stochastic delay systems: Theoretical description and application to a simple model of gene regulation," arXiv:0901.3271, 1–12.

Giudicelli, F., Özbudak, E.M., Wright, G.J. & Lewis, J. [2007] "Setting the tempo in development: An investigation of the zebrafish somite clock mechanism," *PLoS Biol.* **5**, 1309–1323.

Holley, S.A. & Takeda, H., [2002] "Catching a wave: The oscillator and wavefront that create the zebrafish somite seminars," *Cell Dev. Biol.* **13**, 481–488.

Horikawa, H., Ishimatsu, K., Yoshimoto, E., Kondo, S. & Takeda, H. [2006] "Noise-resistant and synchronized oscillation of the segmentation clock," *Nature* **441**, 719–723.

Lewis, J. [2003] "Autoinhibition with transcriptional daley: A simple mechanism for zebrafish somitogenesis oscillator," *Cur. Biol.* **13**, 1398–1408.

Mazzitello, K.I., Arizmendi, C.M. & Hentschel, H.G.E. [2008] "Converting genetic network oscillations into somite spatial patterns," *Phys. Rev. E* **78**, 021906(1)–021906(8).

Morelli, L.G. & Jülicher, F. [2007] "Precision of genetic oscillators and clocks," *Phys. Rev. Lett.* **98**, 228101.

Oates, A.C. & Ho, R.K. [2002] "Hairy/E(spl)-related (Her) genes are central components of the segmentation oscillator and display redundancy with delta/notch signaling pathway in the formation of anterior segmental bounderies in the zebrafish," *Development* **129**, 2929–2946.

Palmeirim, I., Henrique, D., Ish-Horowicz, D. & Pourquie, O. [1997] "Avian hairy gene expression identifies a molecular clock linked to vertebrate segmentation and somitogenesis," *Cell* **91**, 639–648.

Pourquié, O. [2003] "Vertebrate somiogenesis: a novel paradigm for animal segmentation?" *Int. J. Dev. Biol.* **47**, 597–603.

Rida, P.C.G., Minh, N.L. & Jiang, Y. [2004] "A notch feeling of somite segmentation and beyond," *Dev. Biol.* **265**, 2–22.

Saga, Y. & Takeda, H. [2001] "The making of the somite: Molecular events in vertebrate segmentation," *Nat. Rev. Genet.* **13**, 835–845.